

## The Oceanic Microcosm of Particles

Suspended particulate matter, about 1 gram in 100 tons of seawater, plays a vital role in ocean chemistry.

D. Lal

The oceans contain  $1.4 \times 10^9$  cubic kilometers of water, cover more than 71 percent of the earth's surface, and have a mean depth of 3.8 kilometers. The hydrosphere and the atmosphere, the principal fluid reservoirs on the earth, serve as media for the transport and distribution of particles. The total mass of suspended particulate matter in the oceans is estimated to be of the order of  $10^{16}$

in their journey of a few kilometers through the oceanic water column.

The physical and chemical behavior of particles in the oceans influences the chemical and biological makeup of seawater and sediments. Particles thus provide a direct mechanism for the renewal of elements in the sea, in addition to the flux of dissolved elements from rivers. Further, particles of organic and in-

---

*Summary.* Analyses of suspended particulate matter larger than 1 micrometer, filtered from thousands of liters of surface and deep waters during GEOSECS expeditions to the Atlantic and Pacific oceans, have provided new information on the nature and time scales of chemical processes associated with the particles. Trace element and radionuclide data show that particles scavenge trace elements such as Th, Pu, Fe, Pb, and Cu from the ocean column, thereby controlling their concentrations. For other elements, however, particles are a source: carbon and silicon, for example, are introduced at depths as sinking particles dissolve. Studies of both particulate concentrations by filtration of seawater and particulate fluxes by using sediment traps seem necessary to delineate the intricate nature of chemical processes in the oceans.

---

grams, a mere 10 to 20 parts per billion by weight on the average. It is this microcosm of particles that forms the subject of this article. Whether the oceans are merely passageways for particulate matter; whether such an insignificant amount of particles can be of any consequence geophysically, geochemically, or biologically; and what methods have been devised to decipher the roles of the particles in the marine environment will be considered here. I will discuss the diverse types of particles present in the oceans, their concentrations, and the processes that are associated with them

organic materials transported downward into the deep sea are a major food source for benthic organisms.

We now know that the total amount of particulate matter in the oceans is much smaller (1) than it was thought to be only a decade ago (2). Darwin (3) recognized the presence of eolian (wind-transported) material in the remotest ocean areas. This transport mechanism was confirmed by the work of Murray and Renard (4) a half-century later on deep-sea sediments; these authors also pioneered the investigation of cosmic material in deep-sea sediments. Detailed stud-

ies of particulate matter in the oceans by light-scattering were reported by Jerlov in 1953 (5). Measurement of particulate concentrations and size distributions by light-scattering techniques has gained considerable momentum during the past decade (6), especially since the development of the Coulter counter (7). Quantitative studies of the nature and dynamics of particulate matter require direct examination of its size distribution and detailed composition in both seawater (1, 2, 8) and sediments (2, 9). Such observations, coupled with direct studies of atmospheric dust (10) collected between 1955 and 1970, have contributed greatly to our understanding of the origin of marine particulates.

Excellent review articles on particulate matter in seawater are available (11, 12). This article largely focuses on developments that were triggered by the initiation of the international GEOSECS (Geochemical Ocean Sections Study) program (13). In the GEOSECS expeditions (13) to the Atlantic and Pacific oceans emphasis has been placed on determining the distribution in surface and deep waters and the chemical, mineralogical, and radioactive composition of particles. Large-scale sampling of ocean waters and high-resolution optical studies of substantial amounts of collected particulate matter have provided details of the physicochemical and biological processes associated with oceanic particles.

### Geochemical and Biological Significance of Particles

There are four principal sources of particles in the oceans (9-12): (i) suspended matter carried as river load, (ii) airborne dust, (iii) biological particles produced within the oceans, and (iv) cosmic material accreted by the earth. Clearly, the number of questions that a geochemist can ask are many. We may group such inquiries in two categories concerning (i) the geochemical balance of elements, which involves determining

The author is director of the Physical Research Laboratory, Ahmedabad 380009, India, and visiting professor at Scripps Institution of Oceanography, La Jolla, California 92093.

Table 1. Radionuclides useful for the study of particulates (20).

Nuclide	Half-life	Description	Nuclear reaction and source
$^{14}\text{C}$	5730 years	Natural and artificial; cosmic-ray interactions and nuclear weapons	$^{14}\text{N}(n,p)^{14}\text{C}$ ; thermal neutron capture in atmospheric nitrogen
$^{32}\text{Si}$	~ 300 years	Natural; cosmic-ray-produced	$^{40}\text{Ar}(p,x)^{32}\text{Si}$ ; nuclear spallation of atmospheric argon
$^{55}\text{Fe}$	2.7 years	Artificial; from nuclear weapons	$^{56}\text{Fe}(n,2n)^{55}\text{Fe}$ ; energetic neutron-induced reactions with iron in the hardware
$^{210}\text{Pb}$	21 years	Natural; $^{238}\text{U}$ series	$^{226}\text{Ra} \rightarrow$ six steps $\rightarrow$ $^{210}\text{Pb}$ ; produced in situ in seawater and introduced by wet precipitation
$^{226}\text{Ra}$	1620 years	Natural; $^{238}\text{U}$ series	Primarily by diffusion from deep-sea sediments
$^{228}\text{Ra}$	6.7 years	Natural; $^{232}\text{Th}$ series	$^{232}\text{Th} \rightarrow$ $^{228}\text{Ra}$ ; input from rivers and diffusion from sediments
$^{228}\text{Th}$	1.9 years	Natural; $^{232}\text{Th}$ series	$^{228}\text{Ra} \rightarrow$ $^{228}\text{Ac} \rightarrow$ $^{228}\text{Th}$ ; produced in situ in seawater from $^{228}\text{Ra}$
$^{230}\text{Th}$	75,200 years	Natural; $^{238}\text{U}$ series	$^{238}\text{U} \rightarrow$ three steps $\rightarrow$ $^{230}\text{Th}$ ; produced in situ in seawater
$^{232}\text{Th}$	$1.5 \times 10^{10}$ years	Natural	From land, along with detrital material
$^{234}\text{Th}$	24 days	Natural; $^{238}\text{U}$ series	$^{238}\text{U} \rightarrow$ $^{234}\text{Th}$ ; produced in situ in seawater
$^{239}\text{Pu}$	24,300 years	Artificial; nuclear weapons	$^{238}\text{U}(n,\gamma)^{239}\text{Pu}$ ; neutron capture with uranium in weapons

source and sink functions, and (ii) particle dynamics, or processes occurring during transit in the water column. The fluvial and eolian source functions depend on a number of geophysical and meteorological factors (9, 11, 12). Likewise, biological productivity depends on the nature of large-scale oceanic circulation, upwelling, and horizontal mixing by surface current systems which regulate

the supply of nutrients (14). As a result of extensive explorations during the last two decades, we have a fair idea of the standing crop of biological materials and their rate of production (15).

The second task, characterizing particle dynamics, is a difficult one. Particles are present at concentrations of the order of 10 micrograms per kilogram of seawater in the open ocean (> 200 me-

ters); concentrations in surface waters depend on the season and can be as high as a few hundred micrograms per kilogram.

The river load is largely deposited within the continental shelf regions; particles are transported to open ocean areas by surface currents with velocities ranging from 10 to 250 centimeters per second (10 to 200 km/day). Thus, only particles with a Stokes settling velocity of less than  $5 \times 10^{-3}$  cm/sec (corresponding to particles smaller than 5 micrometers) will be transported efficiently to the open ocean. The situation is similar for eolian particles (9-12). Larger land-derived particles are seen in the open ocean, and they must be transported by fast current systems. Biological particles produced in the oceans range in size from about 1 micrometer to 1 millimeter; the concentration of suspended particles larger than 10  $\mu\text{m}$  is however, small. The oceans abound in particles in the size range 1 to 10  $\mu\text{m}$ .

As they sink, particles are removed or reduced in size by grazing by zooplankton (16, 17) or dissolution. The latter is important in the case of calcareous ( $\text{CaCO}_3$ ) and opaline ( $\text{SiO}_2$ ) skeletal materials (18, 19). Particles can also adsorb elements on their surfaces during their descent. The adsorption and desorption processes and their rates can be studied with radionuclides; Table 1 lists some of the important radionuclides and their sources (20).

There have been several reports concerning the role of particles as scavengers for radionuclides from seawater. The presence in marine sediments and on particles filtered from seawater  $^{239}\text{Pu}$ ,  $^{95}\text{Nb}$ ,  $^{55}\text{Fe}$ , and  $^{14}\text{C}$  formed in atmospheric tests of nuclear weapons (21) has been attributed to attachment of these nuclides on settling particles. This explanation has also been given for radioactive disequilibria between chemically

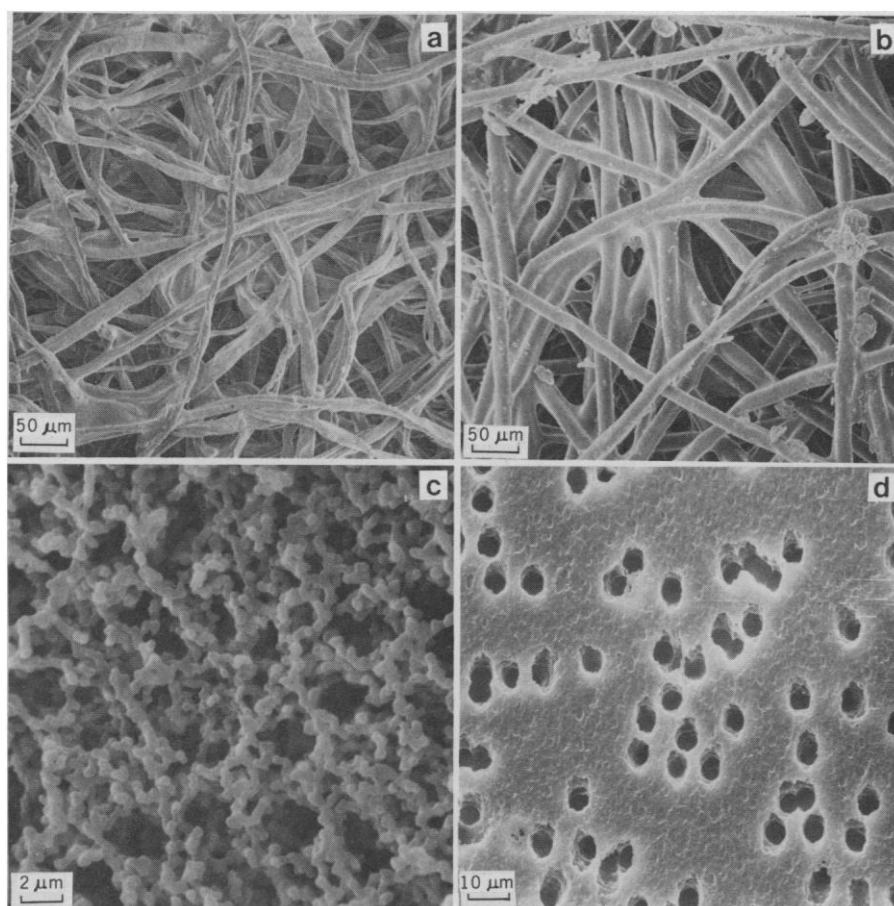
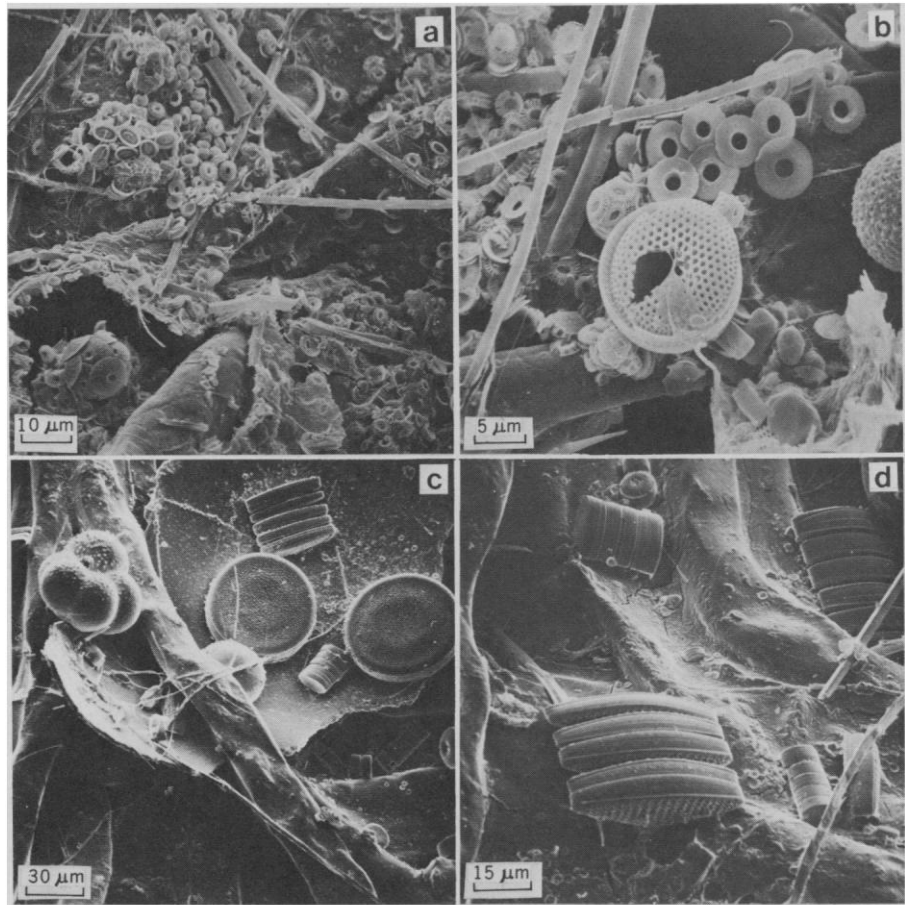


Fig. 1. Scanning electron micrographs of (a) Tamil and (b) Poly fiber filters and (c) Millipore cellulose and (d) Nuclepore screenlike membrane filters. Particles are trapped in the niches between fibers and on the filter surface, as can be seen from Figs. 2, 12, and 13. The membranes act as sieves, obstructing the downward movement of particles above a certain size. In contrast, in the case of filter pads, particles are trapped or stuck on the surfaces of the fibers while water flows freely around the trapped particles.

Fig. 2 (right). Examples of biological particles in surface Pacific waters from (a and b) 40° to 45°N, 160° to 169°E, and (c and d) 57°S, 169°E. The particles in (c) are foraminifera (CaCO<sub>3</sub>) and diatoms (SiO<sub>2</sub>); those in (d) are different species of diatoms. Large number of coccoliths (CaCO<sub>3</sub>) and some radiolarians (SiO<sub>2</sub>) are seen in (a) and (b).



reactive daughter nuclides and their passive parents—for example, the observed disequilibria (22, 23) between <sup>234</sup>Th and <sup>238</sup>U, <sup>210</sup>Pb and <sup>226</sup>Ra, and <sup>228</sup>Th and <sup>228</sup>Ra.

These observations clearly suggest that particles transport radionuclides to great depths in the oceans on time scales short compared to those involved in the large-scale mixing of water. Measurement of these radionuclides at different depths in the ocean makes it possible to study particle dynamics as well as the relevant time scales. There is also evidence that particles release elements to deep waters and may alter the chemical composition of seawater significantly. For example, dissolution of biogenic CaCO<sub>3</sub> and SiO<sub>2</sub> (opaline) particles, besides contributing to dissolved calcium and SiO<sub>2</sub>, also results in the addition to the deep sea of carbon and silicon atoms of higher specific activity from the surface layers. This partly resets the <sup>14</sup>C and <sup>32</sup>Si clocks which are useful for the study of large-scale diffusive and advective mixing processes (24, 25).

Finally, it has been speculated that the wide geographical variations in the concentrations and types of particles present in the oceans could be used to characterize water masses. Plumes with high particle concentrations extending some 2000 m off the bottom between 35° and 40°N have been identified with a pronounced nutrient front in the bottom water. At 35°N and 30°S the sinking of water associated with convergence zones is clearly observed as lobes of high particle concentrations (26).

#### Techniques of Particle Collection and Analysis

The number-size distribution of particles in the oceans follows a steep power law. Therefore, any attempt to study particulate dynamics must be based on quantitative collection of small particles, down to sizes of ~1 μm. Quantitative particle retrieval began with the use of membrane filters (27). Also, the high-speed centrifuging technique (2) has been extensively employed by Soviet scientists in the Indian and Pacific

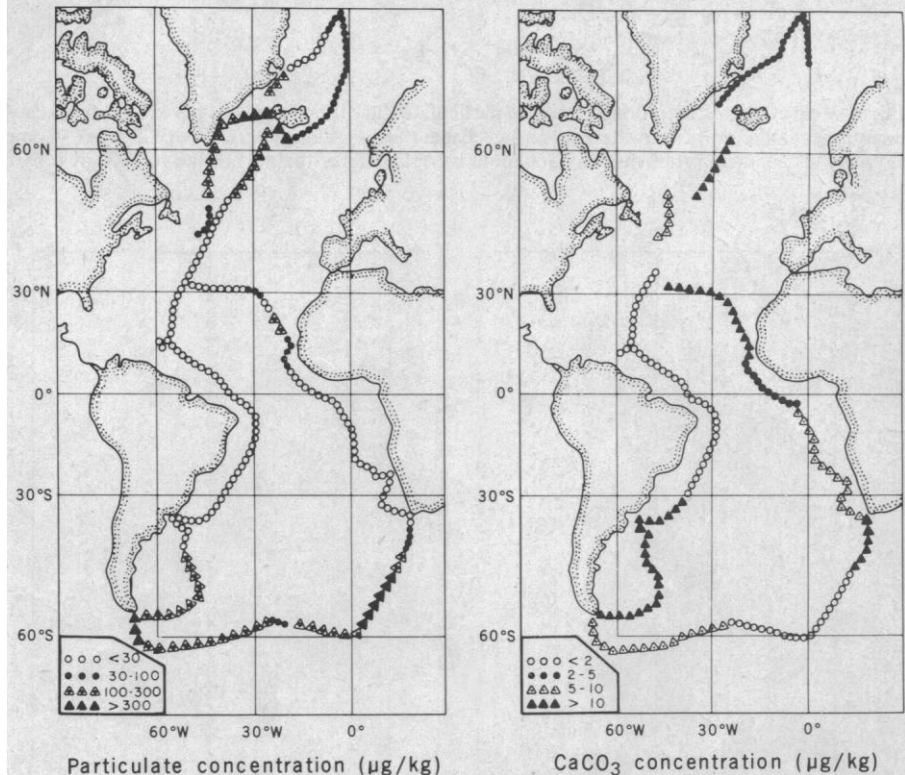


Fig. 3. Measured concentrations (30) of total particulate matter and particulate CaCO<sub>3</sub> are shown along the track of R.V. *Knorr* in surface Atlantic waters. Concentration values (micrograms per kilogram of seawater) are given in four ranges. Each data point represents the results for water filtered continuously between successive GEOSECS stations. Note the high particulate concentrations at high latitudes (> 40°N or > 40°S); these are due to high biological productivity in these regions.

oceans. Generally, 10 to 200 liters of seawater brought on board ship in Niskin bottles or large-volume samplers is processed. With the advent of submersible pumps and pressure switches, it became possible to carry out filtration at depth (28). The data on particulate concentration show that contamination during the sampling and filtration procedure has steadily decreased with time, and the data published during the last few years are generally internally consistent. Because of improvements in collection and

analytical techniques in the last decade, scientists feel confident in processing small amounts of water (20 to 30 liters) and analyzing microgram quantities of suspended matter for their mineral and chemical composition. The analytical tools commonly employed at present include scanning electron microscopy (SEM) coupled with elemental techniques, energy dispersive x-ray fluorescence, instrumental neutron activation analysis (INAA), and atomic absorption spectrophotometry (AAS).

Analysis of the radioactivity of particulate matter has been largely confined to studies of nuclides that are present in seawater in relatively high concentrations, such as  $^{210}\text{Pb}$  (29). The opportunities offered during the GEOSECS expedition stimulated the detailed study of radioactivity and trace element analyses of particulates in the Atlantic and Pacific oceans. Both small (10 to 20 liters) and large (5000 to 20,000 liters) volumes of particulates have been sampled extensively (13). The collected particulates

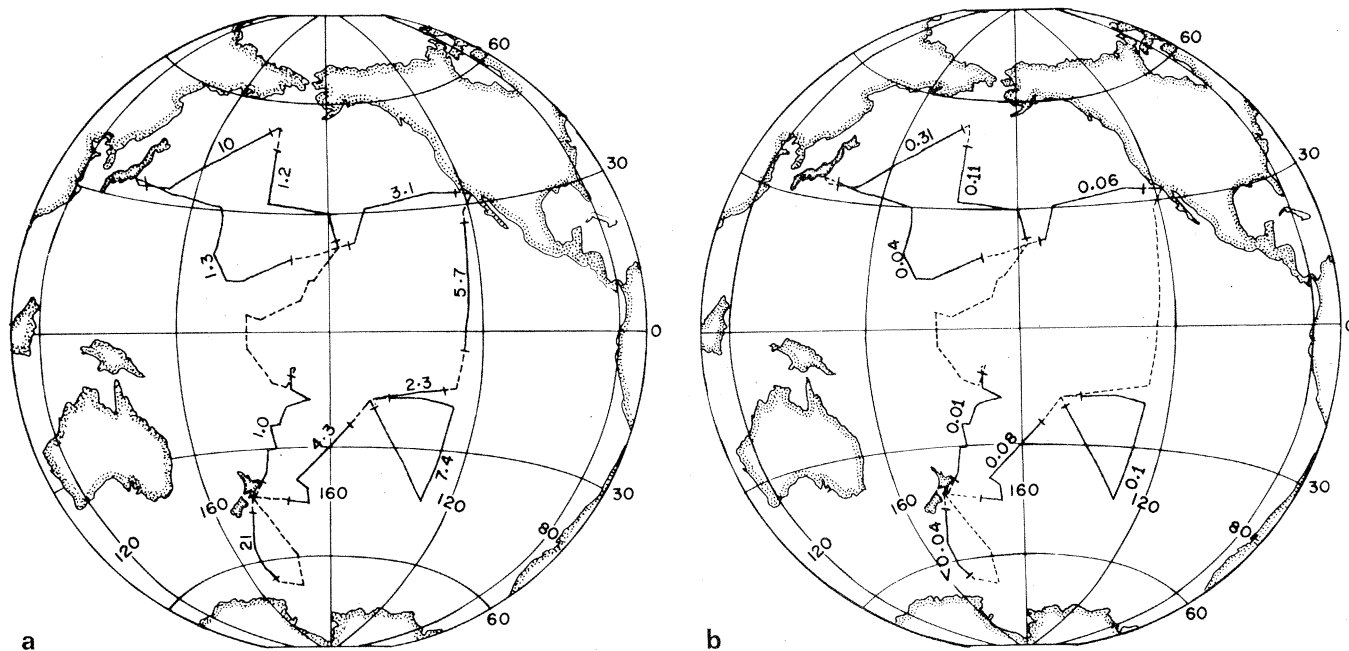


Fig. 4. Measured concentrations (30) of (a) particulate  $\text{CaCO}_3$  (micrograms per kilogram of seawater) and (b) particulate  $^{239}\text{Pu}$  (disintegrations per minute per kilogram of seawater) in surface Pacific waters along the GEOSECS track. Composite filters for several stations were analyzed. Because of technical problems, no data could be obtained for the part of the track shown by dotted lines.

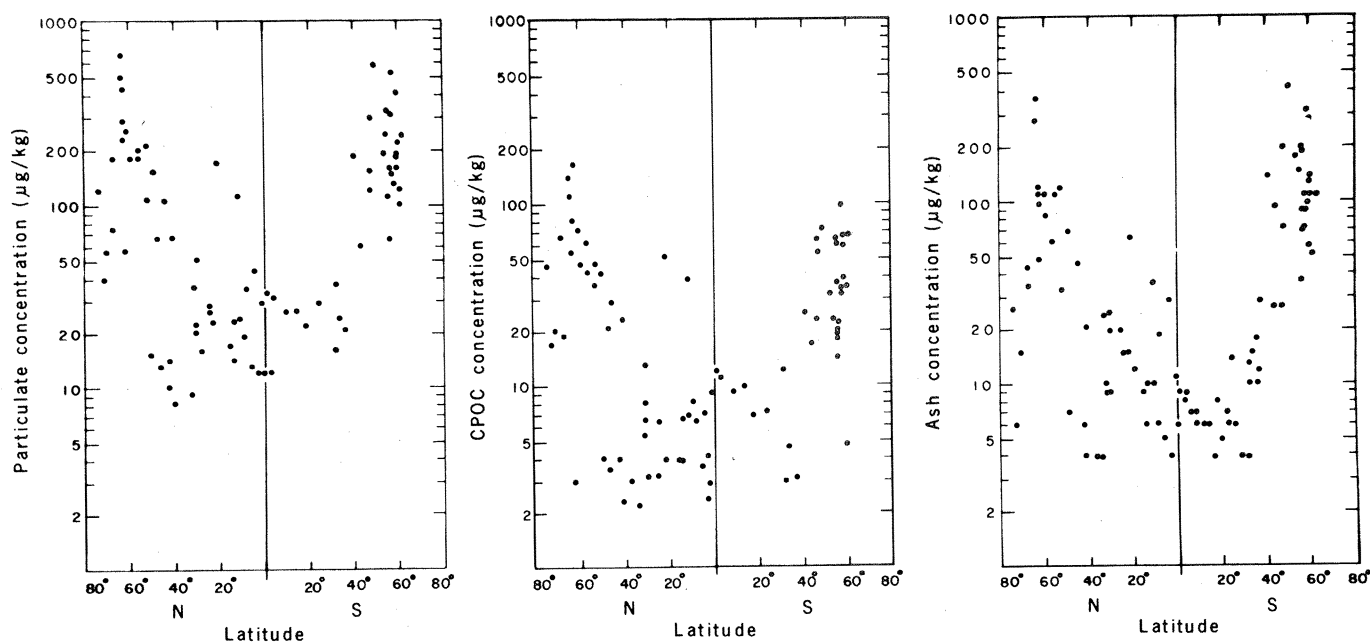


Fig. 5. Scatter diagrams showing concentrations of total particulate matter, calculated particulate organic carbon (CPOC), and ash as a function of latitude for the Atlantic surface waters.

have been analyzed and the concentrations of total particulate matter, ash, particulate organic carbon,  $\text{CaCO}_3$ ,  $\text{SiO}_2$ , and a suite of trace elements including radioactive isotopes have been determined (30, 31).

A severe problem encountered with the use of absolute filters (Millipore cellulose or the Nuclepore membrane) is that the flow rate decreases quickly because of clogging of the pores, so that even in favorable cases (for particle concentrations of the order of 10 to 20  $\mu\text{g}/\text{kg}$ ) it is possible to filter only  $\sim 0.5$  liter per square centimeter of filter area. Thus, even with 29.3-cm filter disks, the largest used so far, only about 300 liters of water (3 to 6 mg of particulates) can be filtered. (The use of prefilters helps only marginally, because small particles which the prefilter does not retain, are the ones mainly responsible for clogging.)

Large-volume filtration of particulates of size  $\geq 1$  to 2  $\mu\text{m}$  became possible with the development of a filter pad-absolute filter combination (30, 31). Figure 1 shows SEM photographs of two types of filter pads used in GEOSECS expeditions (30). How the filter pad operates as an efficient trap for micrometer-size particles is not yet fully understood. Particles are trapped in the small niches between fibers, but the number of such sites available in the filter pad (which is 1.5 mm thick with a fiber diameter of 10 to 15  $\mu\text{m}$ , corresponding to 100 trapping layers) is estimated to be of only of the order of  $10^5$  to  $10^6$  per square centimeter, which should be compared with the typical value of  $10^7$  to  $10^8$  per square centimeter for the 1- $\mu\text{m}$  cellulose or membrane filters. Direct determinations of particle trapping efficiencies, based on studies carried out in ocean waters 80 to 200 km off the coast of San Diego, showed that both Tamil and Poly filters are quantitative compared to 5- $\mu\text{m}$  Millipore and about 60 percent efficient compared to 0.45- $\mu\text{m}$  Millipore. These fiber pads therefore serve not as prefilters, but as highly efficient filters for micrometer-size particles. This is presumably due to the existence of organic coatings on particles in seawater. Marine particles evidently stick efficiently on the fiber surfaces (see Fig. 2), which is consistent with the observation that it is extremely difficult to release trapped particles from a filter pad (or a Millipore filter). The effective number of trapping sites in the Tamil and Poly fiber pads must be about  $10^8$  to  $10^9$  per square centimeter.

During GEOSECS, the large volume filtration setup was mounted in the bow visibility chamber and large volumes of surface waters were filtered while the

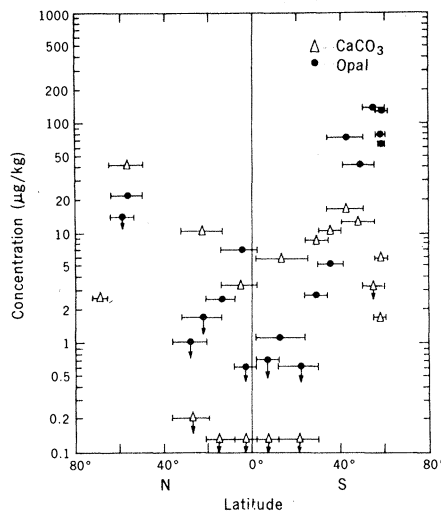


Fig. 6. Latitudinal distribution of particulate  $\text{CaCO}_3$  and  $\text{SiO}_2$  (opal) in surface Atlantic waters (30). Note the similarity to the distribution of total particulate matter (Fig. 3). High concentrations are due to high biological productivity of  $\text{CaCO}_3$  in the northern region and of  $\text{SiO}_2$  in the southern region.

ship was cruising (30). Water volumes of 2,000 to 40,000 liters could be filtered with a 29-cm-diameter fiber pad-Millipore combination in continuous operation for 3 to 5 days.

For deep waters, a self-contained battery-powered filtration system was used (31); the assembly was based on the earlier design of Yentsch, which was successfully used later by several investigators (28). With a 29-cm-diameter Tamil or Poly filter pad (31) coupled to a 1- $\mu\text{m}$  Millipore, the initial filtration rates were 10 to 15 liters per minute. Volumes of 3 to  $7 \times 10^3$  liters could be filtered in 8 hours at depths to 5000 m. For large-volume filtration (32) at depths to 400 m, similar systems have been employed with the pump connected with cables to the ship's power supply. With improvements in fiber pads and power sources, within the next few years it may be possible to extract particles from much larger volumes of deep water, say  $10^5$  to  $10^6$  liters, at much smaller contamination levels.

#### Distribution and Composition of Suspended Particles: GEOSECS Data

The large-scale sampling of particulates during GEOSECS (13) has led to a fairly complete picture of the concentration of particulate matter in surface and deep waters of the Atlantic and Pacific oceans. Four groups carried out the investigations independently with complementary aims. The group from Woods Hole Oceanographic Institution, Woods

Hole, Massachusetts, mapped the lateral and vertical distribution of total suspended matter (33) and determined the elemental composition of the particles by INAA. Scientists from Lamont-Doherty Geological Observatory (LDGO), Palisades, New York, measured the concentration of suspended particles in detailed profiles of samples taken near the bottom in the Atlantic (33) and Pacific oceans. The nature and composition of these particles have been studied at LDGO by combined SEM and energy-dispersive x-ray fluorescence (34). Both water-column and near-bottom samples have also been analyzed for chemical and mineral composition by the group at the Centre des Faibles Radioactivites/CNRS in France by INAA, SEM, and microprobe and at the Université Libre de Bruxelles by light and scanning electron microscopy (34). The group at Physical Research Laboratory determined concentrations and compositions of suspended matter in surface and deep waters by quantitative filtration of particulates  $\geq 1$  to 2  $\mu\text{m}$  from  $\geq 10^4$  liters of surface water and  $>10^3$  liters of deep water (30, 31). Since large amounts of suspended matter were trapped, it was possible to determine the concentrations of a host of radionuclides and to obtain fairly precise estimates of the detrital and biogenic contributions to the total particulate matter (TMP). (Henceforth, by particulate  $\text{CaCO}_3$  or particulate  $^{226}\text{Ra}$  concentration I mean the concentration of  $\text{CaCO}_3$  or  $^{226}\text{Ra}$  in the particulate phase.) The various studies referred to above were carried out in the Atlantic and Pacific oceans; however, laboratory investigations are still under way and the published results to date are mostly for the Atlantic Ocean.

A great diversity of trapped particles has been observed. Figure 2 shows four scanning electron micrographs of particulate biogenic forms that are abundant in surface waters. The samples of oceanic suspended material are vastly different from atmospheric dust samples, because of the great diversity of morphologies of the numerous planktonic species. The artistic diversity is not purely aesthetic; it is in part a necessity (35) dictated by the requirement that the sinking rates must be slow enough not only to allow a minimal absorption of essential nutrients but also to secure the necessary time for the particles to be brought back into the euphotic zone through vertical movements.

*Global distribution of suspended matter in surface waters.* Results based on continuous large-volume filtration of surface waters along the GEOSECS tracks

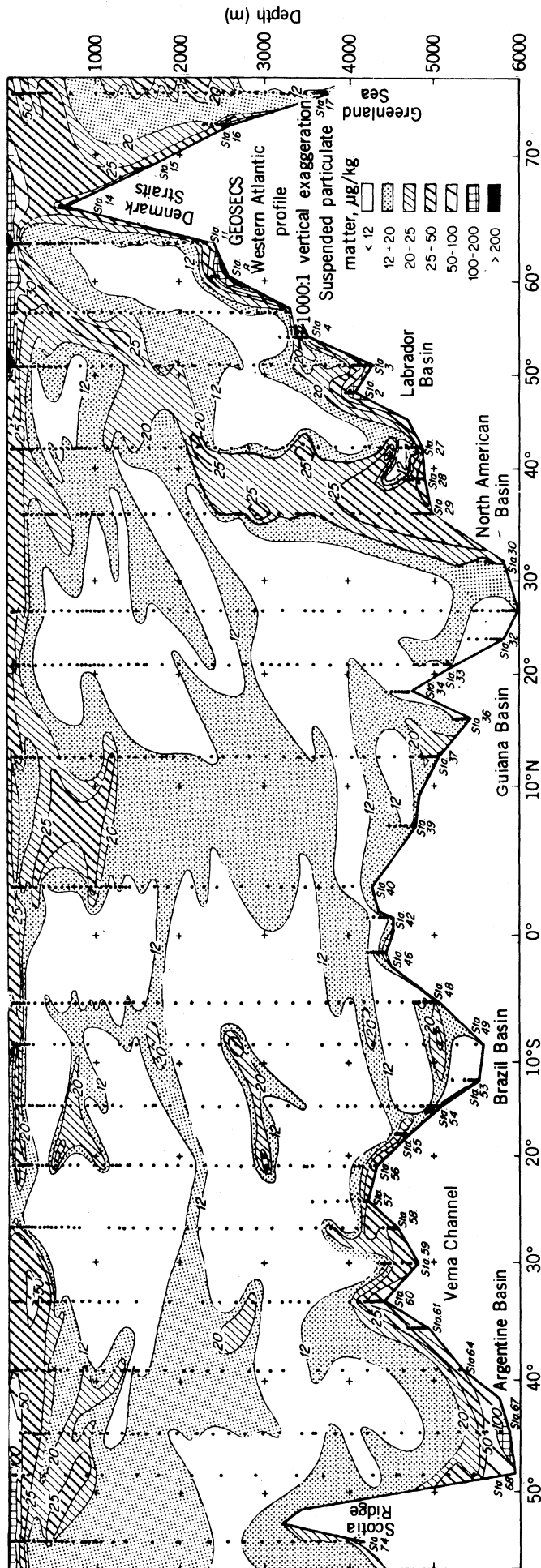


Fig. 7. Isocontours for concentrations of total suspended matter in Atlantic waters measured by the Woods Hole and Lamont-Doherty groups (33).

are illustrated in Figs. 3 and 4. Besides the concentration of TPM, particulate  $\text{CaCO}_3$ , particulate  $\text{SiO}_2$ , the total amount of "ash" (comprising calcareous, opaline, and detrital matter) obtained by heating the filters to 400° to 425°C, and particulate organic carbon calculated from weight loss on ignition (CPOC) have been determined.

The concentrations of TPM and  $\text{CaCO}_3$  along GEOSECS tracks in the Atlantic Ocean are given in Fig. 3. Values range from 10 to 600  $\mu\text{g}/\text{m}^3$ ; with high values generally occurring at latitudes above 40°N or 40°S. A characteristic feature of the distribution of TPM is its latitudinal near-symmetry, with minimum values around the equator. The latitudinal distributions of TPM and two of its major components, CPOC and ash, are shown in Fig. 5. Ash constitutes 30 to 70 percent of TPM; high values occur at high southern latitudes (> 40°S), where TPM is composed mainly of biogenic opal (Fig. 6). The  $\text{CaCO}_3$  concentration in surface Atlantic waters is nearly uniform (Fig. 6), averaging about 10  $\mu\text{g}/\text{kg}$ . Calculated particulate organic carbon constitutes about 25 percent of TPM, with concentrations ranging from <10 to 166  $\mu\text{g}/\text{kg}$ . The large geographical variations in the concentrations and composition of biogenic materials that comprise ~80 percent of TPM are consistent with known oceanographic features—upwelling and horizontal circulation patterns.

The contribution of detrital phases (largely aluminosilicates) to TPM can be estimated from its aluminum content. The data of Krishnaswami and Sarin (36) indicate that the detrital phase constitutes about 2 percent of TPM in the Atlantic (range, 0.3 to 9 percent). [Particulate aluminum concentrations in surface waters vary by more than an order of magnitude, 30 to 800  $\mu\text{g}/\text{kg}$  (36, 37), with high values along the glacial and trade wind transport regions.]

Total particulate concentrations are low in the surface waters of the Pacific compared to the Atlantic. The ash and  $\text{CaCO}_3$  values range from 5 to 80 and from 1 to 20  $\mu\text{g}/\text{kg}$ , respectively (Fig. 4). From a comparison of ash and  $\text{CaCO}_3$  values, I conclude that, on the average, TPM values in surface waters are two to three times lower in the Pacific than in the Atlantic.

*Depth distribution of suspended matter.* The concentration of TPM at various depths has been measured (33, 34) at intervals of 100 to 200 m in the upper water column and at intervals of tens of meters near the bottom in the western Atlantic Ocean from 75°N to 52°S (Fig. 7); extensive data are also available for the near-bottom regions (26). Similar data, based on 30-liter samples, will soon become available for the Pacific Ocean, including analyses of some of the samples for several trace elements (such as Al, Ca, Sr, Ba, and Mg). Limited data on ash and  $\text{CaCO}_3$  are now available for the Pacific, based on analyses of 3000- to 7000-liter samples (31).

In deep Atlantic waters (> 500 m) TPM concentrations lie in the range 10 to 20  $\mu\text{g}/\text{kg}$  (excluding regions of nepheloid layers); in contrast to values in the near-surface waters of 30 to 50  $\mu\text{g}/\text{kg}$  between 30°N and 30°S and >100  $\mu\text{g}/\text{kg}$  at latitudes > 40°. At middle depths highs are associated with recently formed deep water; values of 20 to 30  $\mu\text{g}/\text{kg}$  are found for new deep waters formed by convective overturn in the Labrador Sea, at the subtropical convergences in the North and South Atlantic, and at the Antarctic polar front (33). A concentration of 10  $\mu\text{g}/\text{kg}$  is typical for the rest of the "clear" deep waters of the Atlantic.

At about 35°N and 30°S lobes of high particle concentrations are associated with convergence zones (33). The nepheloid layer (6, 26, 33) is clearly evident at high lati-

tudes and in regions characterized by a deep western boundary current. High TMP values are found in the bottom layer identified as the Denmark Strait overflow water.

The  $\text{CaCO}_3$  concentrations at depths of  $> 500$  m in the Atlantic, based on measurements of calcium (33), are 1 to  $2.5 \mu\text{g/kg}$ . These values are comparable to those for the Pacific (31). It should be noted that very high values are observed for the South Pacific, in both surface and deep waters.

An interesting feature reported by the LDGO and French groups (34) is the existence in deep waters of several opaque particles, barite and several iron minerals (such as goethite), and colored sausage-like particles possibly of industrial origin. Barite and gypsum are presumably authigenic; the others are of terrestrial or anthropogenic origin. Figure 8 shows a photomicrograph of a particle which owes its origin to automobile exhaust.

*Radioactivity of particulates in surface and deep waters.* The radioactive isotopes  $^{234}\text{Th}$ ,  $^{230}\text{Th}$ ,  $^{228}\text{Th}$ ,  $^{226}\text{Ra}$ ,  $^{239}\text{Pu}$ ,  $^{210}\text{Pb}$ ,  $^{14}\text{C}$ , and  $^{32}\text{Si}$  were measured in composite surface filters from successive stations along the GEOSECS tracks. Observed concentrations of  $^{234}\text{Th}$ ,  $^{228}\text{Th}$ , and  $^{226}\text{Ra}$  in suspended phases are presented in Fig. 9 for surface Atlantic waters. Data are available for particulate  $^{239}\text{Pu}$  in surface waters of the Atlantic and Pacific and in deep Pacific waters (Fig. 10). Additional data, not presented here, are also available (30, 31) for  $^{210}\text{Pb}$ ,  $^{230}\text{Th}$ , and  $^{232}\text{Th}$  in particulates from surface and deep waters and for  $^{32}\text{Si}$  in surface waters.

In deep Pacific waters (data are not available for the Atlantic) the particulate concentrations of  $^{234}\text{Th}$ ,  $^{210}\text{Pb}$ , and  $^{239}\text{Pu}$  generally amount to  $< 20$  percent of their total activity in the water. The concentration of particulate  $^{230}\text{Th}$  increases nearly linearly with depth, reaching a maximum value of  $\sim 2 \times 10^{-4}$  disintegrations per minute per kilogram, about 0.01 percent of the theoretical secular equilibrium value (with respect to  $^{234}\text{U}$ ). The particulate concentration of  $^{239}\text{Pu}$  is greatest at a depth of  $\sim 1000$  m.

The latitudinal distribution of radionuclides (Figs. 9 and 10) is similar to that of suspended matter (TPM, CPOC, and ash). However, the reasons for the observed distribution are different. We are dealing here with radioisotopes from widely different sources (see Table 1). The  $^{239}\text{Pu}$  comes from nuclear weapon tests;  $^{234}\text{Th}$ ,  $^{230}\text{Th}$ , and  $^{228}\text{Th}$  are produced in situ in seawater; and  $^{232}\text{Th}$  primarily comes from land. The low values

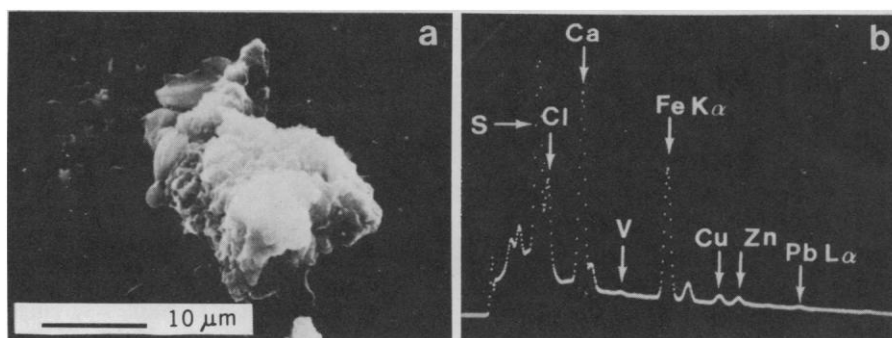


Fig. 8. (a) Particle found at a depth of 500 m in the Atlantic Ocean ( $33^{\circ}15'N$ ,  $53^{\circ}33'W$ ); it appears as a black sausage when viewed in transmission with an optical microscope. The object contains significant concentrations of S, Cl, Ca, Fe, V, Cu, Zn, and Pb, based on the x-ray spectrum shown in (b). Jedwab and Chesslet (56) attribute this particle to automobile exhaust.

at the equator in the case of  $^{234}\text{Th}$  and  $^{226}\text{Ra}$  must be ascribed to lower amounts of particulate matter in these waters. However, the distribution of  $^{239}\text{Pu}$  primarily reflects its atmospheric fallout pattern (Fig. 10). The availability of radioisotopes from different sources makes it possible to delineate the principal geochemical and geophysical processes that regulate their concentrations of these nuclides (30).

#### Particle Dynamics: Theoretical

##### Considerations

In the upper layers of the oceans ( $< 200$  m), an important process for detrital and biogenic phases is grazing by zooplankton, which recycles and aggregates both types of materials in an important but highly complex manner (16, 17, 31, 38, 39). In transit through the water column, the particles are also subject to dissolution as well as growth by adsorption (40, 41).

In this section I discuss simple theoretical relationships for a population of particles with a specified spectral size distribution, considering dissolution and adsorption effects as particles are transported downward due to gravitational settling.

Particle size distributions in the oceans are usually well represented by the relation

$$dN/dr = A r^{-b} \quad (1)$$

where  $N$  is the number of particles of radius  $r$  and  $A$  and  $b$  are constants. Measurements of TPM and measurements of forams and diatoms are consistent with Eq. 1, with values of  $b$  usually between 4 and 5 (38, 42, 43).

Particles in suspension are transported out of a water mass by gravitational (Stokes) settling. This process dominates

the transport of particles  $> 1 \mu\text{m}$  with densities  $> 1.5 \text{ g/cm}^3$  through distances of the order of 1 km and with an eddy diffusivity of  $1 \text{ cm}^2/\text{sec}$  (40, 44, 45).

The total surface area,  $S$ , mass,  $M$ , and mass flux,  $F$ , across a layer, due to particles of radius between  $r_1$  and  $r_2$  having a size distribution given by Eq. 1 are

$$S(r_1 - r_2) \propto r^{-(b-3)} \quad \left| \begin{array}{l} r_2 \\ r_1 \end{array} \right. \quad (2)$$

$$M(r_1 - r_2) \propto r^{-(b-4)} \quad \left| \begin{array}{l} r_2 \\ r_1 \end{array} \right. \quad (3)$$

$$F(r_1 - r_2) \propto r^{-(b-6)} \quad \left| \begin{array}{l} r_2 \\ r_1 \end{array} \right. \quad (4)$$

The slope  $b$  determines the size range of particles responsible for various processes. Adsorption of trace elements depends on available surface area. The in situ regeneration rate, termed the  $J$  flux (grams per kilogram per second) by Craig (25), involves  $M$  and  $F$ . With  $b$  in the range 4 to 5, particles between 1 and  $10 \mu\text{m}$  primarily contribute to trace element adsorption onto aluminosilicate and other detrital grains, and also to the  $J$  flux. Particles  $< 1 \mu\text{m}$  are usually not important, since for particles to be effective in bringing about chemical changes the mass flux has to be appreciable ( $S$  varies as  $r^{-1}$  or  $r^{-2}$ , but  $F$  varies as  $r$  or  $r^2$ ). Also, as noted above, small particles essentially follow the motion of water molecules if the eddy diffusivity is  $\geq 1 \text{ cm}^2/\text{sec}$ . Thus, for practical purposes, particles  $< 0.5 \mu\text{m}$  may be considered as in solution. Marine particulate matter may therefore be defined as suspended particles of size  $> 0.5 \mu\text{m}$ . Parsons (12) has similarly defined particulate organic carbon as particles larger than  $0.5$  to  $1.0 \mu\text{m}$ .

In theoretical formulations to date it has been assumed that the particles are solid spheres. This is an oversimplification, since besides generally

being irregular in shape, biological particles have hollow structures with perforations, cups, caps, and so on (16, 17, 35). If particle morphologies are known, settling velocities can be calculated (35, 40), but the diversity of forms renders any such attempt tedious and impractical. Also, the effective densities of these particles are not known with any precision (45). Finally, theoretical considerations of particle dynamics involve a knowledge of the rate constants for reactions such as dissolution and adsorption. Our knowledge of these is limited; and there are large uncertainties because of the presence of organic coatings on the particles (46). Nevertheless, it is instructive to carry out order-of-magnitude

calculations. Several papers have recently appeared on the subject of dissolution of calcareous and opaline particles during their transit through the seawater column (40, 43, 47, 48), and I will summarize their main conclusions.

*Fates of biogenic particles.* Changes in the size of a particle transiting through the water column depend on its initial size. Theoretical relationships have been derived for the case of Stokes settling, with and without an advection velocity. The radius of the particle as a function of depth is given by

$$B(r_0^3 - r^3) - 3 U_a(r_0 - r) - 3 \epsilon(z - z_0) = 0 \quad (5)$$

where  $r$  is the particle radius at depth  $z$ ; the subscript 0 refers to  $z = 0$ , and  $B$  is the constant of proportionality for the Stokes settling velocity ( $U$ ) relation,  $U = B r^2$ . The upwelling (advection) velocity of water is  $U_a$ . The rate of dissolution of the particle,  $\epsilon$  (centimeters per year), has been assumed to be independent of depth. If  $U_a = 0$

$$r = r_0 \left[ 1 - \frac{3\epsilon(z - z_0)}{B r_0^3} \right]^{1/3} \quad (6)$$

The rate of change in radius of a particle is  $dr/dt = -\epsilon$ , independent of particle radius, but the change in radius of a particle in traversing a depth  $z - z_0$  is sensitively dependent on the initial ra-

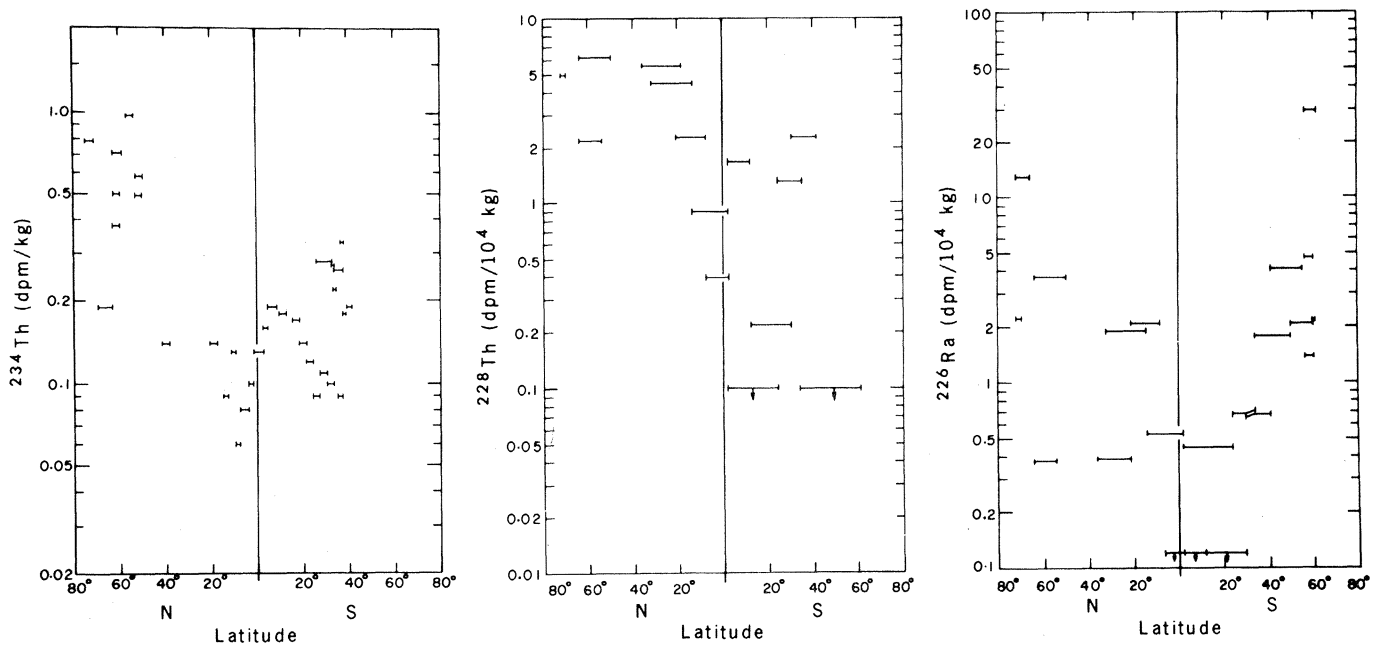


Fig. 9. Concentrations (disintegration per minute per kilogram of seawater) of particulate  $^{234}\text{Th}$ ,  $^{228}\text{Th}$ , and  $^{226}\text{Ra}$  as a function of latitude in surface waters of the Atlantic Ocean (30). The results refer to composite samples collected between stations (see Fig. 3).

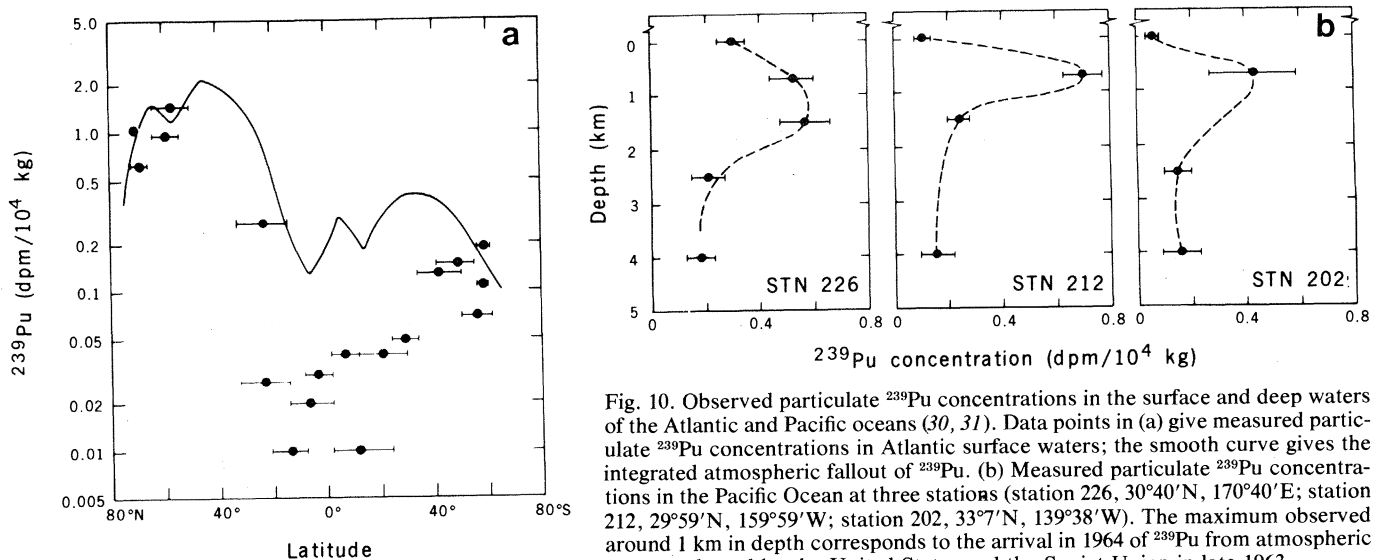


Fig. 10. Observed particulate  $^{239}\text{Pu}$  concentrations in the surface and deep waters of the Atlantic and Pacific oceans (30, 31). Data points in (a) give measured particulate  $^{239}\text{Pu}$  concentrations in Atlantic surface waters; the smooth curve gives the integrated atmospheric fallout of  $^{239}\text{Pu}$ . (b) Measured particulate  $^{239}\text{Pu}$  concentrations in the Pacific Ocean at three stations (station 226,  $30^{\circ}40'\text{N}$ ,  $170^{\circ}40'\text{E}$ ; station 212,  $29^{\circ}59'\text{N}$ ,  $159^{\circ}59'\text{W}$ ; station 202,  $33^{\circ}7'\text{N}$ ,  $139^{\circ}38'\text{W}$ ). The maximum observed around 1 km in depth corresponds to the arrival in 1964 of  $^{239}\text{Pu}$  from atmospheric tests conducted by the United States and the Soviet Union in late 1963.

dus. It follows from Eq. 6 that  $dr/r = -(\epsilon/B)r^{-3}dz$ . Thus, over small distances, the fractional change in radius varies inversely as  $r^3$ . (The same is true for particles which dissolve only partly in going through the entire oceanic column.)

The behavior of Eq. 6 is schematically shown in Fig. 11, a and b. If the initial particle radius,  $r_0$ , is large compared to  $[B/3\epsilon(z - z_0)]^{1/3}$  the particle plummets rapidly through the oceanic column with essentially no change in size (Fig. 11a); a smaller particle undergoes appreciable dissolution (Fig. 11b), as expected by the  $r^{-3}$  dependence.

The time to total dissolution of a particle of initial radius  $r_0$  is  $(r_0/\epsilon)$ . Two interesting situations arise, as shown in Fig. 11, c and d. If advection is not considered, the particle ends its journey at depth  $z$  by dissolving entirely at  $z - z_0 = Br_0^3/3\epsilon$ . In the presence of advection, the direction of motion is reversed, and the particle moves upward along  $U_a$ ; the reversal depth,  $z_r$ , is given by (40)

$$z_r = \frac{2B}{3\epsilon} \left( \frac{U_a}{B} \right)^{3/2} + \frac{Br_0^3}{3\epsilon} - \frac{U_a r_0}{\epsilon} \quad (7)$$

The hypothetical particle in Fig. 11d will then dissolve completely after traversing an upward distance given by

$$z_r - z_{r=0} = 2(U_a^3/B)^{1/2}/3\epsilon \quad (8)$$

Equation 8 is independent of the initial particle size. Further, as particles diminish in size and slow down, their residence time in the water increases and hence their number concentration increases (40, 43). The value  $z_r - z_{r=0}$  lies between 10 cm and 10 m based on the known values for the parameters:  $U_a = 1.4 \times 10^{-5}$  cm/sec,  $\epsilon = 1.5 \times 10^{-5}$  cm/year for calcite for depths less than 3500 m and  $2 \times 10^{-3}$  cm/year for radiolarians, and  $B = 7.27 \times 10^3$  cm<sup>-1</sup> sec<sup>-1</sup> for particles of density 1.5 g/cm<sup>3</sup>. Hence each particle of initial radius between, say,  $r_1$  and  $r_2$  generates a layer with a small thickness,  $z_r - z_{r=0}$ , independent of  $r_0$ , between  $z_{r_1}$  and  $z_{r_2}$ . The radius at reversal,  $(U_a/B)^{1/2}$ , is calculated to be 0.44  $\mu$ m. For such particles transport by diffusion becomes important, and therefore the depth interval  $z_r - z_{r=0}$  will be larger in practice but it will still remain finite.

Such conditions (Fig. 11d) are applicable for calcite and radiolarian particles of initial radius (at  $z = 0$ ) less than 5 and 20  $\mu$ m, respectively, and are expected to give rise to particles in the micrometer size range. Thus, upwelling can generate nepheloid layers of biogenic (or other)

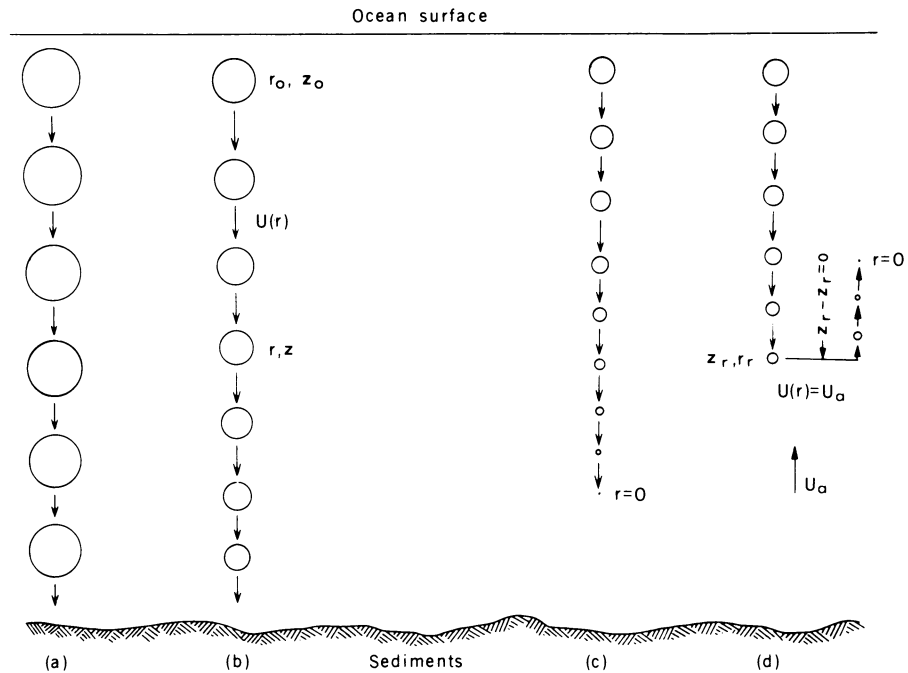


Fig. 11. Fates of biogenic particles as they settle through an oceanic column of water. Larger particles settle faster (Stokes velocity,  $U \propto r^2$ ) and are subject to less chemical erosion. Cases (a) and (b) illustrate the expected  $r^{-3}$  dependence on percentage change in radius. Cases (c) and (d) show particles that are initially small enough that they do not survive through the water column. If an upwelling velocity  $U_a$  is considered, the direction of motion of the particle is reversed at a particular value of radius. The distance traveled to the point of complete dissolution is small (see text). This process can give rise to layers of high particle concentrations in the deep ocean similar to the observed nepheloid layers (6).

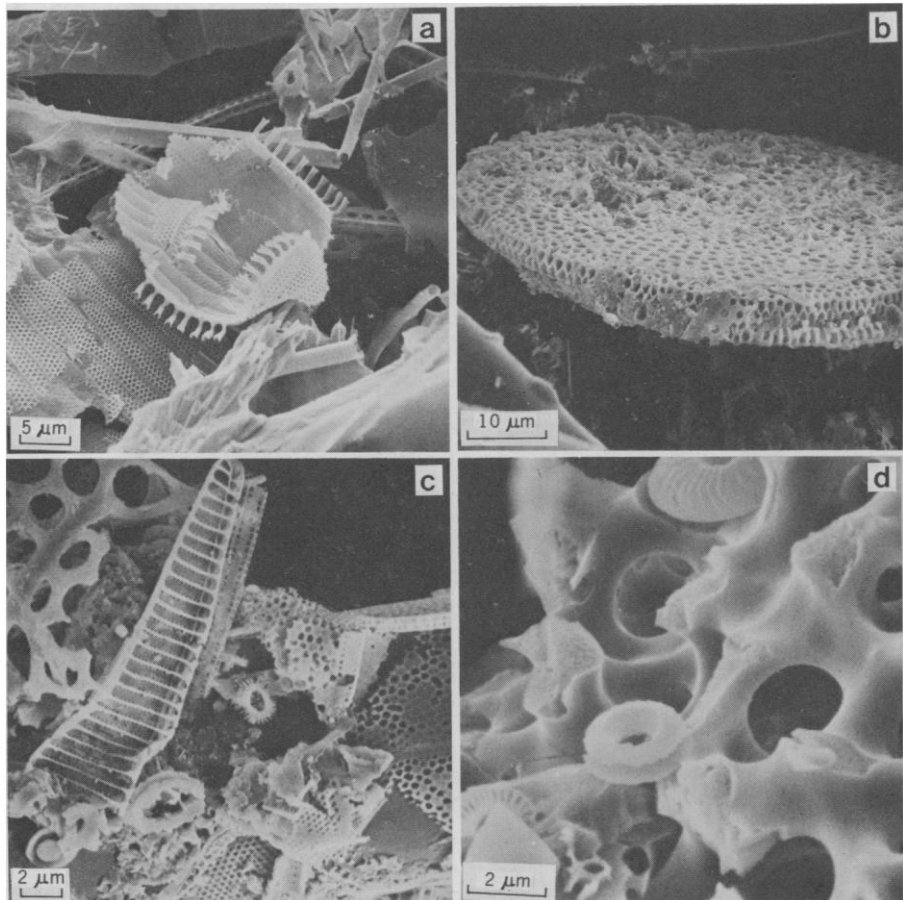


Fig. 12. Scanning electron micrographs showing free coccoliths (d) and several varieties of siliceous tests (a to c). The samples were collected from a depth of 4300 m in the Pacific Ocean (5°N, 124°W). The skeletal materials have been heavily corroded.

particles that undergo dissolution in seawater (40).

Theoretical calculations have been carried out for Stokes settling of a population of particles of different sizes (43, 47). These calculations have provided approximate estimates of the regeneration rates (that is,  $J$  flux) for carbon and silicon and highlight the importance of fragmentation in determining the steady-state number-size spectra of biogenic particles in the deep ocean.

*Adsorption of trace elements onto clay and other detrital particles.* Our present state of understanding of chemical processes associated with clay and other detrital phases limits us to considerations of adsorption of elements onto the surfaces of these particles during their transport through the water column. This is of particular relevance here since sufficient GEOSECS data are available for several radionuclides. Processes such as desorption and coagulation of particles must be operative at significant levels in the ocean (39-41, 45).

The first observations on the marked disequilibrium of  $^{234}\text{Th}$  in the oceans led

Bhat *et al.* (22) to propose a simplified particle transport model in which it was assumed that 100 percent of the  $^{234}\text{Th}$  activity was present in suspended phases. Subsequently, however, it was found that only 10 to 20 percent of the activity resides in particulate phases. The more realistic model of Krishnaswami *et al.* (31) for the thorium isotopes, analogous to that of Somayajulu and Craig (49) for  $^{210}\text{Pb}$ , considers the general case of a parent-daughter pair where the parent is chemically passive, existing entirely in dissolved form. Similar calculations have been performed by Tsunogai and co-workers (50).

The expected concentrations of the daughter nuclide,  $\chi$ , in particulate phases are given by the relation

$$\frac{d\chi}{dt} = -S \frac{d\chi}{dz} + C\psi - \chi\lambda \quad (9)$$

Here  $S$  is the effective particle settling velocity ( $U - U_a$ ) and  $C$  is the concentration of dissolved daughter nuclide of half-life =  $0.693/\lambda$ . The first-order attachment coefficient,  $\psi$ , relates the particulate concentrations of the daughter

nuclide to its rate of production from the parent. If the concentration of dissolved parent nuclide of half-life  $0.693/\lambda_p$  is  $C_p$ , we obtain

$$C_p\lambda_p = C(\lambda + \psi) \quad (10)$$

In practice, the parameters  $C_p$ ,  $\psi$ , and  $S$  are depth-dependent. If the concentrations of dissolved and particulate parent and daughter are measured as a function of depth, the parameters of interest,  $S$  and  $\psi$ , can be determined. The coefficient  $\psi$  is related to the residence time,  $\tau_\psi$ , of the nuclide in the seawater, against removal by attachment to particles. (Since  $\psi$  would depend on the particle concentration, it would be expected to be depth-dependent.)

### Comparison of GEOSECS Data with Theory

The  $J$  flux of trace elements to the deep waters is one of the important manifestations of particle dynamics; it has to be understood explicitly to properly use  $^{14}\text{C}$  and  $^{32}\text{Si}$  to determine the parameters of large-scale water circulation (24, 25). The reverse phenomenon, the  $J$  efflux—that is, removal of dissolved elements at all depths by adsorption on the sinking particles—becomes important for understanding the budget of several trace elements such as Th, Pb, and Cu (24, 25, 51). It should be noted that many of the trace elements appear as discrete particles composed largely or entirely of Cu, Ba, Zn, Ti, and others (34).

*J flux.* Photomicrographs of biogenic particles in deep waters clearly indicate that small particles undergo appreciable dissolution in going through a few kilometers of seawater. The calcareous and opaline skeletal materials illustrated in Fig. 12 provide some support for this statement. In fact, the larger particles in deep water are generally found to be well preserved in the deepest samples. In the final analysis, the  $J$  flux for calcium and silicon must depend on the smallest dimension of the particles. In a perforated disk-shaped object, for example, the effect of dissolution will at first be to thin down the skeleton. The skeleton will then fragment into many pieces which, being small, will undergo much faster dissolution (Fig. 11). The opaline spicules likewise must undergo a complex dissolution process, fragmenting at first at the weak points and then dissolving quickly thereafter. Biological material is also broken up in the upper layers of the ocean by grazing, part of the material being directly rejected by the zooplankton and part incorporated in fecal materi-

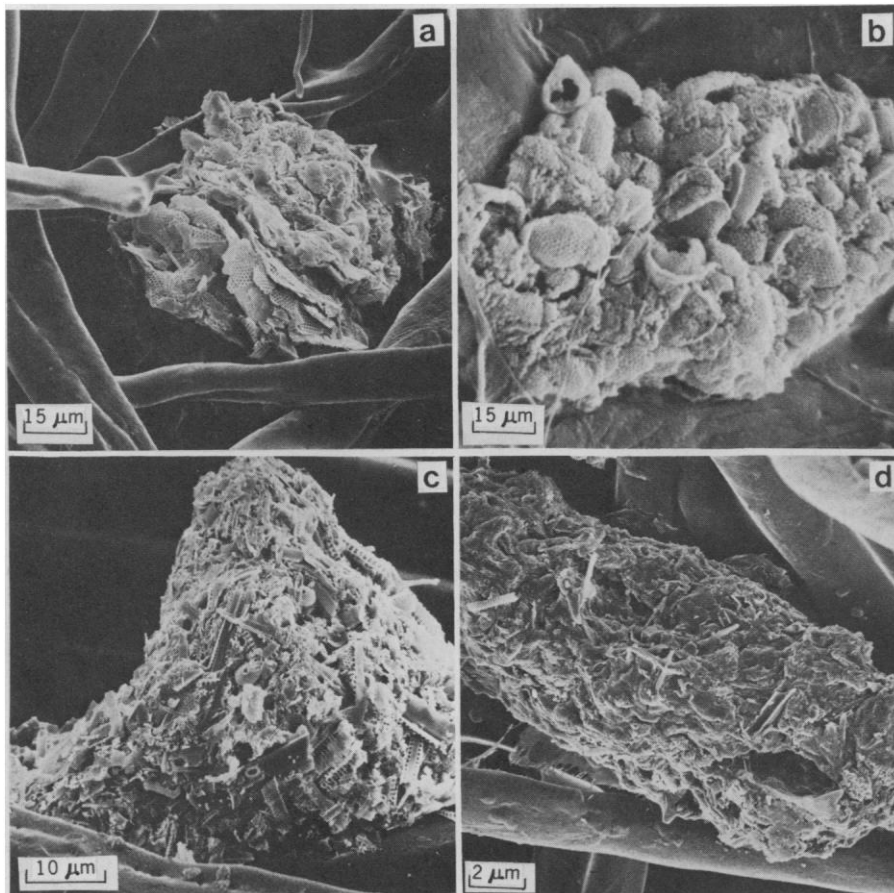


Fig. 13. Scanning electron micrograph showing fecal pellets containing diverse biogenic skeletal materials (primarily diatoms, some free diatoms, and some free coccoliths) and some detrital phases. The samples were collected from the Pacific Ocean. Note that most of the biological material, except in (b), exists in a highly fragmented state. The aggregate in (b) is from the surface; the material in (a) to (c) is from 4300 m in depth.

al. Fecal pellets may or may not release trapped material during their transit through the ocean water column (16, 17). Figure 13 shows fecal pellets containing material in a highly fragmented state from both surface and deep waters. The photographic evidence suggests that the large biological particles undergo a two-step process in contributing to the  $J$  flux: first fragmentation, either by dissolution or grazing, and then dissolution by chemical erosion; dissolution is significant only for particles of radius smaller than  $10 \mu\text{m}$ .

The particle size distribution in the size range 1 to  $10 \mu\text{m}$  does not seem to change with depth for either the total particle population or the calcareous and siliceous materials (38, 42, 43). In surface waters the concentration of particles decreases rapidly (by a factor of 2 in 50 to 60 m). Lerman *et al.* (38) have interpreted these data as indicating that in the upper layers suspended materials are removed indiscriminately, and independently of particle size, by bulk grazing. However, there is evidence that herbivore grazing in the upper layers is methodic (52). In either case, the constancy of the size spectrum in deep waters must be due to the fragmentation process; a dramatic change in size distribution would be expected (Fig. 11) if only dissolution took place.

If we compare theoretical estimates of the  $J$  flux with the experimental data, the agreement is reasonable. For  $\text{SiO}_2$  and  $\text{CaCO}_3$ , Lerman and Lal (47) theoretically estimate integrated values of  $25 \pm 2$  and  $8 \pm 2 \mu\text{mole cm}^{-2} \text{ year}^{-1}$  for the depth interval 1 to 5 km in the Pacific Ocean. In the case of carbon (53), the total flux would be four to five times larger than that based on  $\text{CaCO}_3$ . The predicted depth dependence in the regeneration rate of  $\text{SiO}_2$  agrees reasonably well with estimates of the  $J$  flux by Fiadeiro (54) based on a three-dimensional analysis of GEOSECS data on dissolved silica in the Pacific.

$J$  *efflux*. The rate of attachment onto particles can be deduced for several elements. Of particular interest are elements for which radionuclide pairs are available as tracers—for example,  $^{234}\text{Th} : ^{238}\text{U}$  and  $^{210}\text{Pb} : ^{226}\text{Ra}$ . In these cases the behavior of thorium and lead can be precisely delineated on the basis of model calculations. The activity of the daughter nuclide relative to its parent in the particulate phase depends on the settling velocity of the particle,  $S$ , and the attachment coefficient,  $\psi$ ,

$$\frac{\chi\lambda}{C_p\lambda_p} = \frac{\psi}{\lambda + \psi} (1 - e^{-\lambda z/S}) \quad (11)$$

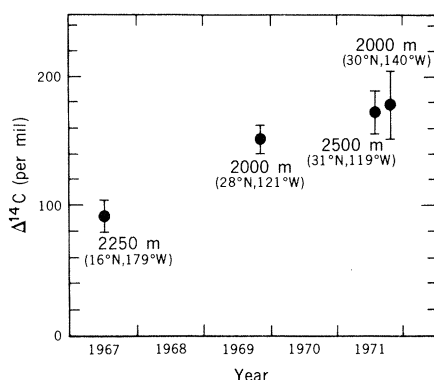


Fig. 14. Observed  $\Delta^{14}\text{C}$  values of carbon in particulate  $\text{CaCO}_3$  at depths of 2000 to 2500 m in the Pacific Ocean from 1967 to 1971 (55). Such high values are expected only for recently formed biogenic calcareous particles; the  $\Delta^{14}\text{C}$  values in surface waters increased because of nuclear weapons testing from about  $-50$  per mil before 1950 to 300 per mil during 1973 (on the same scale). Combining information on the post-1950 variations of  $\Delta^{14}\text{C}$  in dissolved carbonate in surface waters with  $\Delta^{14}\text{C}$  values in particulate  $\text{CaCO}_3$  at depths, one can estimate the average settling velocities of  $\text{CaCO}_3$  particles (21).

Equation 11, a solution of Eq. 9, has been used to study the measured particulate concentrations of  $^{234}\text{Th}$  and  $^{230}\text{Th}$ . These thorium isotopes have widely different half-lives that can be used to determine  $\psi$  and  $S$ , assuming that they are independent of depth and that  $\psi(^{230}\text{Th}) = \psi(^{234}\text{Th})$ .

For  $^{234}\text{Th}$ , Eq. 11 becomes

$$\frac{\chi\lambda}{C_p\lambda_p} \approx \frac{\psi}{\lambda + \psi} \quad (12)$$

when  $z \gg S/\lambda$ . The activity ratio is independent of  $z$ , as also observed experimentally (31).

For  $^{230}\text{Th}$ , Eq. 12 becomes

$$\frac{\chi\lambda}{C_p\lambda_p} \approx \frac{\psi}{\lambda + \psi} \cdot \frac{\lambda z}{S} \quad (13)$$

The linear depth dependence expected for the long-lived isotope  $^{230}\text{Th}$  is actually observed (31). Equations 12 and 13 yield values for  $\psi$  and  $S$  of  $\approx 8 \times 10^{-8} \text{ sec}^{-1}$  and  $\approx 10^{-3} \text{ cm/sec}$ , respectively (31). This value of  $\psi$  is quite consistent with the absolute particulate concentration of  $^{230}\text{Th}$ . Tsunogai and co-workers (50) obtained a value for  $S$  of  $1.1 \times 10^{-3} \text{ cm/sec}$  based on  $^{234}\text{Th}$  data for surface waters  $< 100 \text{ m}$  in good agreement with the estimate based on  $^{230}\text{Th}$  data for deep waters.

Particle settling velocities can also be deduced from observed  $^{55}\text{Fe}$  and  $^{239}\text{Pu}$  activities in particulates, which show a maximum at depths of 750 to 1000 m (see Fig. 10) (31). The values of  $S$  estimated in this way lie in the range  $3$  to  $6 \times 10^{-4}$

$\text{cm/sec}$  (21, 31, 55); they are somewhat lower than the value based on  $^{230}\text{Th}$  data; but the agreement is quite good considering the scatter in the particulate  $^{230}\text{Th}$  data.

The settling velocities deduced have been for inorganic detrital materials—aluminosilicates and ferric oxide particles, on which Th, Pu, and Fe are expected to be adsorbed; these elements may also be adsorbed onto particulate organic carbon. Settling velocities of  $\text{CaCO}_3$  particles have also been estimated on the basis of observations of their excess  $^{14}\text{C}$  activities (corresponding to  $\text{CaCO}_3$  particles formed in surface waters after nuclear testing): the data (Fig. 14) lead to the value  $S = 2.7 \pm 0.35 \times 10^{-3} \text{ cm/sec}$ . [Carbon-14 activities observed at depths of 2000 to 2500 m during 1971 (Fig. 14) correspond to the values observed in surface waters during 1968 and 1969.] This value for  $S$  is greater than that based on observations of removal of  $^{230}\text{Th}$ ,  $^{239}\text{Pu}$ , and  $^{55}\text{Fe}$  by particles which is to be expected since the latter nuclides will be scavenged by small particles, adsorption being a strong function of available surface area (compare Eqs. 2 and 3).

## Conclusions

The new information available about the distribution of marine suspended matter, primarily as a result of GEOSECS expeditions to the Atlantic and the Pacific, has revolutionized our thinking about chemical cycles in the oceans. The physical, chemical, and biological problems connected with particles are too numerous for a coherent summary to be given here. Instead, I will simply list the salient features.

1) Throughout the oceans, biological particles dominate the detrital phases.

2) In surface waters ( $< 100 \text{ m}$ ), organic matter comprises 30 to 70 percent of total particulate matter. The hard skeletal phases of the marine organisms,  $\text{CaCO}_3$  and  $\text{SiO}_2$ , together comprise about 25 to 50 percent of total particulate matter.

3) In surface waters, the global distributions of minerals and biological particles show a pronounced latitudinal effect, and are nearly symmetric in some cases about an equatorial minimum. Also, the particulate concentrations of the radionuclides  $^{234}\text{Th}$ ,  $^{228}\text{Th}$ ,  $^{226}\text{Ra}$ , and  $^{239}\text{Pu}$  are lowest at equatorial latitudes. However, the reasons for the equatorial minimum are different for different radionuclides.

4) As particles transit through the water column, some elements are added to

seawater (in dissolved form), whereas some are removed from solution. The in situ addition and removal of trace elements—termed the  $J$  flux and the  $J$  efflux, respectively—modify the composition of seawater appreciably in the case of several elements. Corroded biological particles retrieved from depths (Fig. 12) provide testimony of the  $J$  flux for calcium, carbon, and silicon. The high enrichment factors for several radionuclides and elements provide evidence for a significant  $J$  efflux due to particles. The  $J$  efflux is the primary mechanism controlling the residence times of several trace elements, such as Th, Pu, Fe, Pb, and Cu, in seawater.

5) In surface waters, suspended materials are recycled by the zooplankton. By this mechanism biological particles are fragmented; and some fragmented and whole biological particles are removed from surface waters, packaged as fecal pellets (16, 17). The fecal pellets are the principal food supply for benthic forms and also provide a mechanism for the safe delivery of biological particles to the ocean floor. The role of fecal pellet formation and its relevance to the paradoxes that one faces in attempting to interpret the observations of coccoliths in deep waters and in sediments have been discussed by Honjo (17). Quantitative estimates of the  $J$  flux and  $J$  efflux or of sedimentation to the ocean floor due to fecal pellet processes are not yet possible.

6) Despite the number of processes occurring within the oceans, the particle size distribution remains approximately independent of depth. Corrosive fragmentation of particles in deep waters seems to be an important step contributing to  $J$  flux; particles dissolve rapidly once they are broken up in parts (see Fig. 11).

The methodology for studying particle dynamics that I have discussed here has limitations. An examination of suspended matter in the oceans is necessarily biased toward smaller particles, which settle slowly and thus have a longer residence time. If an appreciable fraction of detrital material enters the oceans as aggregates, or a significant amount of particulate matter in the oceans is packaged in large fecal pellets, a considerable flux of both detrital and biological particles would be missed in any calculations based on observations of suspended matter (16, 17, 45). To judge the magnitude of the large-particle transport mode, one has to study the outgoing flux at different depths in the oceans, using traps or pans (16, 17). Thus, processes occurring with-

in the oceans are properly studied through observations of suspended matter obtained by filtering seawater, but for studies of flux to the sediments, supplementary observations of samples obtained with particle traps or pans must be used.

I have discussed the various phenomena associated with the sparse population of particles in seawater. The situation is somewhat analogous to a deck of marked cards: the oceanographer knew all along that the deck was marked, but he has only recently begun to understand how the apparently invisible marks are used. Further studies of oceanic suspended material, collected by both filters and traps, are warranted by the data. A number of radionuclides of different source functions and half-lives are available for a quantitative study of processes in the oceans. Comparisons of data from the Atlantic and the Pacific are extremely valuable because of the marked differences that are observed in the concentrations of detrital phases and biological particles in the suspended matter in these oceans.

#### References and Notes

1. M. B. Jacobs and M. Ewing, *Science* **163**, 380 (1969); J. E. Harris, thesis, Texas A & M University (1971).
2. A. P. Lisitzin, *Oceanogr. Res.* **2**, 71 (1960); E. M. Emelyanov *Okeanologiya* **2** (No. 4), 664 (1962); Ye. I. Gordeyev, *Dokl. Akad. Nauk SSSR* **149** (No. 1), 181 (1963); A. P. Lisitzin, *Sedimentation in the World Ocean* (Society of Economic Paleontologists and Mineralogists, Tulsa, Okla., 1972), pp. 85–178.
3. C. Darwin, *Q. J. Geol. Soc. London* **2**, 26 (1846).
4. J. Murray and A. F. Renard, *Rep. Sci. Results Voyage H.M.S. Challenger* (1891), vol. 3.
5. N. G. Jerlov, *Rep. Swed. Deep Sea Exped.* **3** (part 3), 71 (1953); *Optical Oceanography* (Elsevier, New York, 1968).
6. M. Ewing and E. M. Thorndike, *Science* **147**, 1291 (1965); S. Eittreim, M. Ewing, E. M. Thorndike, *Deep Sea Res.* **16**, 613 (1969); S. L. Eittreim and M. Ewing, in *Suspended Solids in Water*, R. J. Gibbs, Ed. (Plenum, New York 1974), p. 213; P. E. Biscaye and S. L. Eittreim, *Mar. Geol.* **23**, 155 (1977).
7. R. W. Sheldon and T. R. Parsons, *A Practical Manual on the Use of the Coulter Counter in Marine Research* (Coulter Electronics Co., Toronto, 1967); K. L. Carder, G. F. Beardsley, H. Pak, *J. Geophys. Res.* **72**, 5070 (1971).
8. D. J. P. Swift, J. R. Schubel, R. W. Sheldon, *J. Sediment. Petrol.* **42**, 122 (1972).
9. R. W. Rex and E. D. Goldberg, *Tellus* **10**, 153 (1958); G. Arrhenius, in *The Sea*, M. N. Hill, Ed. (Wiley, New York, 1963), vol. 3, pp. 655–718; P. E. Biscaye, *Bull. Geol. Soc. Am.* **76**, 803 (1965); R. J. Gibbs, *ibid.* **78**, 1203 (1967); J. J. Griffin, H. Windom, E. D. Goldberg, *Deep Sea Res.* **15**, 666 (1968); E. D. Goldberg, *Comments Earth Sci. Geophys.* **1**, 117 (1971).
10. E. D. Goldberg, *Trans. N.Y. Acad. Sci.* **27**, 7 (1964); J. M. Prospero, E. Bonatti, C. Schubert, T. N. Carlson, *Earth Planet. Sci. Lett.* **9**, 287 (1970); C. E. Junge, *Air Chemistry and Radioactivity* (Academic Press, New York, 1963), pp. 111–208.
11. T. R. Parsons, *Prog. Oceanogr.* **1**, 203 (1963); J. P. Riley and R. Chester, in *Introduction to Marine Chemistry* (Academic Press, London, 1971), pp. 311–318; R. Chester, in *The Changing Chemistry of the Oceans*, D. Dyrssen and D. Jagner, Eds. (Wiley, New York, 1972), pp. 291–306; D. W. Menzel, in *The Sea*, E. D. Goldberg, Ed. (Wiley, New York, 1974), vol. 5, pp. 659–678; R. Chester and J. H. Stoner, *Nature (London)* **240**, 552 (1972).
12. T. R. Parsons, in *Chemical Oceanography*, J. P. Riley and G. Skirrow, Eds. (Academic Press, London, ed. 2, 1975), vol. 2, pp. 365–383.
13. The GEOSECS program is a cooperative detailed investigation of the geochemical properties of seawater. It was initiated in 1967 and is funded by the National Science Foundation. Expeditions have been completed to the Atlantic (July 1972 to April 1973) and Pacific (August 1973 to June 1974) oceans. See H. Craig, *Earth Planet. Sci. Lett.* **23**, 63 (1974); \_\_\_\_\_ and K. K. Turekian, *ibid.* **32**, 217 (1976). Collected GEOSECS papers are published in *J. Geophys. Res.* **36**, 7641 (1970); *Earth Planet. Sci. Lett.* **16**, 47 (1972); *ibid.* **23**, 63 (1974); *ibid.* **32**, 217 (1976).
14. W. S. Broecker, *Chemical Oceanography* (Harcourt Brace Jovanovich, New York, 1974), pp. 3–29; K. K. Turekian, *Oceans* (Prentice-Hall, Englewood Cliffs, N.J., 1968), pp. 73–105.
15. O. J. Koblenz-Mishke, V. V. Volkovinsky, J. G. Kabanova, in *Scientific Exploration of the South Pacific*, W. S. Wooster, Ed. (National Academy of Sciences, Washington, D.C., 1970), pp. 183–193.
16. H.-J. Schrader, *Science* **174**, 55 (1971); T. J. Smayda, *Oceanogr. Mar. Biol. Annu. Rev.* **8**, 353 (1970).
17. S. Honjo, *Mar. Micropaleontol.* **1**, 65 (1976).
18. M. N. A. Peterson, *Science* **154**, 1542 (1966); W. H. Berger, *ibid.* **156**, 383 (1967).
19. W. H. Berger, *ibid.* **159**, 1237 (1968); D. C. Hurd, *Earth Planet. Sci. Lett.* **15**, 411 (1972).
20. A. B. Joseph, P. F. Gustafson, I. R. Russell, E. A. Sheuert, H. L. Volchok, A. Templin, in *Radioactivity in the Marine Environment*, A. H. Seymour, Ed. (National Academy of Sciences-National Research Council, Washington, D.C., 1971), p. 6; H. L. Volchok, V. T. Bowen, T. R. Folsom, W. S. Broecker, E. A. Sheuert, G. S. Bien, in *ibid.*, p. 42; C. M. Lederer, J. M. Hollander, I. Perlman, *Table of Isotopes* (Wiley, New York, 1968), p. 594.
21. V. E. Noshkin and V. T. Bowen, in *Radioactive Contamination of the Marine Environment* (International Atomic Energy Agency, Vienna, 1973), p. 671; S. Krishnaswami, *Proc. Indian Acad. Sci. Sect. A* **80**, 116 (1974); M. Gross, *Nature (London)* **216**, 670 (1967); B. L. K. Somayajulu, D. Lal, S. Kusumgar, *Science* **166**, 1397 (1969); P. M. Williams, J. A. McGowan, M. Stuiver, *Nature (London)* **227**, 375 (1970).
22. S. G. Bhat, S. Krishnaswami, D. Lal, Rama, W. S. Moore, *Earth Planet. Sci. Lett.* **5**, 483 (1969).
23. E. Matsumoto, *Geochim. Cosmochim. Acta* **39**, 205 (1975); H. Craig, S. Krishnaswami, B. L. K. Somayajulu, *Earth Planet. Sci. Lett.* **17**, 295 (1973); W. S. Broecker, A. Kaufman, R. M. Trier, *ibid.* **20**, 35 (1973).
24. D. Lal, *J. Oceanogr. Soc. Jpn.* **20**, 600 (1962).
25. H. Craig, *J. Geophys. Res.* **74**, 5491 (1969).
26. D. W. Spencer, P. E. Biscaye, P. L. Sachs, R. E. Ackermann, *Eos* **54**, 306 (1973); P. E. Biscaye and S. L. Eittreim, in *Suspended Solids in Water*, R. J. Gibbs, Ed. (Plenum, New York, 1974), p. 227; R. A. Feely, *Mar. Chem.* **3**, 121 (1976).
27. E. D. Goldberg, M. Baker, D. L. Fox, *J. Mar. Res.* **11**, 233 (1952); R. J. Gibbs, in *Suspended Solids in Water*, R. J. Gibbs, Ed. (Plenum, New York, 1974), p. 3; E. T. Baker, R. N. Sternberg, D. A. McManus, in *ibid.*, p. 155; P. E. Biscaye and S. L. Eittreim, in *ibid.*, p. 227.
28. J. C. Laird, D. P. Jones, C. S. Yentsch, *Deep Sea Res.* **14**, 251 (1967); D. W. Spencer and P. L. Sachs, *Mar. Geol.* **9**, 117 (1970).
29. B. L. K. Somayajulu and H. Craig, *Earth Planet. Sci. Lett.* **32**, 268 (1976).
30. S. Krishnaswami, D. Lal, B. L. K. Somayajulu, *ibid.*, p. 403.
31. \_\_\_\_\_, R. F. Weiss, H. Craig, *ibid.*, p. 420.
32. J. K. B. Bishop and J. N. Edmond, *J. Mar. Res.* **34**, 181 (1976); \_\_\_\_\_, D. R. Ketten, *Deep Sea Res.*, in press.
33. P. C. Brewer, D. W. Spencer, P. E. Biscaye, A. Hanley, P. L. Sachs, C. L. Smith, S. Kadar, J. Fredericks, *Earth Planet. Sci. Lett.* **32**, 393 (1976). The particulate samples were collected by filtering 4 to 20 liters of seawater on board the ship through Nuclepore filters of pore size 0.4 and 0.6  $\mu$ m.
34. P. E. Biscaye and P. Varlamoff, *Eos* **56**, 371 (1975); in *Benthic Processes and the Geochemistry of Interstitial Waters*, abstracts of papers presented at the Joint Oceanographic Assembly, Edinburgh, Scotland (Food and Agriculture Organization, Rome, 1976); R. Chesselet, J. Jedwab, C. Darcourt, F. Dehairs, *Eos* **57**, 255 (1976); R. Chesselet, D. Spencer, P. Biscaye, in *Ocean Mixing Symposium*, abstracts of papers presented at the Joint Oceanographic Assembly, Edinburgh, Scotland (Food and Agriculture Organization, Rome, 1976); R. Chesselet, C. Dar-

- court-Rieg, J. Jedwab, *Eos*, **54**, 333 (1973).
35. W. H. Munk and G. A. Riley, *J. Mar. Res.* **11**, 215 (1952).
  36. S. Krishnaswami and M. M. Sarin, *Earth Planet. Sci. Lett.* **32**, 430 (1976).
  37. P. G. Brewer, D. W. Spencer, M. L. Bender, *Eos* **65**, 308 (1974); R. Chester and J. H. Stoner, *Nature (London)* **255**, 50 (1975).
  38. A. Lerman, K. L. Carder, P. R. Betzer, *Earth Planet. Sci. Lett.*, in press.
  39. F. G. Lowman, T. R. Rice, F. A. Richards, in *Radioactivity in the Marine Environment* (National Academy of Sciences, Washington, D.C., 1971), p. 161; E. K. Duursma, in *ibid.*, p. 147.
  40. D. Lal and A. Lerman, *J. Geophys. Res.* **78**, 7100 (1973); A. Lerman, D. Lal, M. F. Dacey, in *Suspended Solids in Water*, R. J. Gibbs, Ed. (Plenum, New York, 1974), p. 17; R. Wollast, in *The Sea*, E. D. Goldberg, Ed. (Wiley, New York, 1974), vol. 5, p. 359.
  41. G. A. Parks, in *Chemical Oceanography*, J. P. Riley and G. Skirrow, Eds. (Academic Press, London, ed. 2, 1975), pp. 241-308.
  42. S. Krishnaswami and D. Lal, *Spec. Publ. Mar. Biol. Assoc. India* (1973), pp. 139-148.
  43. D. Lal and A. Lerman, *J. Geophys. Res.* **80**, 423 (1975); *ibid.*, p. 4563. The number-size spectrum (Eq. 1) has often been erroneously referred to as a hyperbolic distribution, following a remark by H. Bader [*J. Geophys. Res.* **75**, 2822 (1970)] that on linear scales, Eq. 1 plots somewhat like a hyperbola and is a hyperbola when the exponent  $b$  is 1 and the asymptotes are used as axes. However, the value of  $b$  lies in range 4 to 5, and there seems to be no advantage in making an analogy with the special case of the hyperbola. Equation 1 is aptly described as a power-law relation.
  44. J. C. Brun-Cottan, *J. Geophys. Res.* **81**, 1601 (1976).
  45. I. N. McCave, *Deep Sea Res.* **22**, 491 (1975).
  46. K. E. Chave, *Science* **148**, 1723 (1965).
  47. A. Lerman and D. Lal, *Am. J. Sci.* **277**, 238 (1977).
  48. J. R. V. Zaneveld, thesis, Oregon State University (1972).
  49. B. L. K. Somayajulu and H. Craig, *Earth Planet. Sci. Lett.* **32**, 268 (1976).
  50. Y. Nozaki and S. Tsunogai, *Earth Planet. Sci. Lett.* **32**, 313 (1976); S. Tsunogai, Y. Nozaki, M. Minagawe, S. Yamamoto, in *Oceanography of the Bering Sea*, D. W. Hood and E. J. Kelley, Eds. (Institute of Marine Science, University of Alaska, Fairbanks, 1974).
  51. H. Craig, *Earth Planet. Sci. Lett.* **23**, 149 (1974).
  52. G. A. Paffenhofer and J. D. H. Strickland, *Mar. Biol.* **5**, 97 (1970); G. R. Harbison and R. W. Gilmer, *Limnol. Oceanogr.* **21**, 517 (1976).
  53. Y. H. Li, T. Takahashi, W. S. Broecker, *J. Geophys. Res.* **74**, 5507 (1969).
  54. M. E. Fiadeiro, thesis, University of California, San Diego (1975).
  55. D. Lal and B. L. K. Somayajulu, *Limnol. Oceanogr.* **22**, 55 (1977).
  56. J. Jedwab and R. Chesslet, unpublished report.
  57. Thanks are due to H. Craig, S. Krishnaswami, A. Lerman, B. L. K. Somayajulu, D. Spencer, and R. Weiss for many useful scientific discussions and to members of the GEOSECS Operations Group for the shipboard operations. I am grateful to P. E. Biscaye and P. G. Brewer for helpful criticism. This work could not have been completed without the assistance and useful suggestions from H. Craig and S. Krishnaswami.

## Beef Production Efficiency

The efficiency of beef production can be improved by applying knowledge of nutrition and breeding.

Allen Trenkle and R. L. Willham

Today in the United States, questions are being asked about the role of animals in food production because they consume feed grains that could otherwise be used directly for human consumption. However, livestock, especially cattle,

well as a source of high quality protein that nutritionally complements basic grain diets.

Because ruminants utilize many materials not digestible by simple-stomached animals, including man, they have at-

---

*Summary.* In the production of high quality protein, feed grains will continue to be used to finish cattle for market as long as economics dictates. Production systems could be developed that would make ruminant animals less competitive with humans for feed grains, but the costs of instituting such programs would be prohibitive. Sufficient genetic variation exists either between or within breeds for the cattle population to be adapted to new management programs and for current methods of beef production to be significantly improved.

---

have been an integral part of grain production agriculture for thousands of years. They have served as power; refuse scavengers; a means of transportation of the grain after consumption; producers of fertilizer; a highly flexible food reserve; sources of fiber, leather, and biochemicals; harvesters of forage from adjacent nontillable land areas; as

tracted attention in several recent reviews (1). Ruminants are not as efficient as some other species in converting feed grains and oil seed meals to meat. Whether agriculture becomes limited to crop production in the future depends on the ability of the livestock industry, especially that part of the industry utilizing ruminants, to integrate efficient production systems into total agriculture output, and on the potential for improve-

ment in animal production through the application of research. In this article we discuss research developments in nutrition and genetics which may improve the efficiency of meat production from beef cattle, currently the most conspicuous consumers of feed grains.

### Efficiency of Protein Production

Efficiency is the production of a desired effect with a minimum of input, or it can be considered as the ratio of output to input. There is no single expression that describes the overall efficiency of the beef industry, much less that of animal agriculture. The inputs and desired outputs for a breeding herd are quite different from those for animals used for slaughter. The desired output for breeding animals is reproduction, whereas that for market animals is production of high quality beef. Economically, inputs of labor, capital, land, and population size are most important. Around four animals exist in the breeding herd per market animal produced (2). To assess the outputs or inputs of animal agriculture in the same units is impossible. For feedlot cattle, the efficiency of protein production may be expressed as protein produced over protein consumed, but there is no efficiency ratio that can be used to include the value of insulin extracted from the pancreas. To simplify the discussion, biological efficiency will be considered as product nutrients per feed nutrient.

Changes in body composition can have a marked effect on efficiency. Fatty tissue contains more energy per gram than muscle tissue, so that a given quantity of feed will produce less fat than lean muscle. On a caloric basis the accumula-

---

The authors are professors of animal science, Iowa State University, Ames 50011.